JACS
JOURNAL OF THE AMERICAN CHEMICAL SOCIETY
Article
pubs.acs.org/JACS

Oxazines: A New Class of Second-Order Nonlinear Optical Switches

Pierre Beaujean,[†] Flavie Bondu,[‡] Aurélie Plaquet,[†] Jaume Garcia-Amorós,[§] Janet Cusido,[§] Françisco M. Raymo,[§] Frédéric Castet,[‡] Vincent Rodriguez,[‡] and Benoît Champagne*[,†]

[†]University of Namur, Laboratoire de Chimie Théorique, Unité de Chimie Physique Théorique et Structurale, rue de Bruxelles, 61, B-5000 Namur, Belgium

[‡]Université de Bordeaux, Institut des Sciences Moléculaires (ISM), UMR 5255 CNRS, Cours de la Libération 351, F-33405 Talence Cedex, France

[§]Laboratory for Molecular Photonics, Department of Chemistry, University of Miami, 1301 Memorial Drive, Coral Gables, Florida 33146-0431, United States

Supporting Information

ABSTRACT: A combined experimental−theoretical investigation has revealed that oxazine-based compounds are multiaddressable, multistate, and multifunctional molecular switches exhibiting contrasts of both linear and second-order nonlinear optical properties. The switching properties are particularly large when the substituent is a donor group. In this study, the cleavage of the C−O bond at the junction of the indole and oxazine cycles (of the closed **a** forms) is acido-triggered, leading to an open form ($\mathbf{b}^+$) characterized by larger first hyperpolarizabilities (β_{HRS}) and smaller excitation energies than in the closed form. These results are confirmed and interpreted utilizing *ab initio* calculations that have been carried out on a broad set of compounds to unravel the role of the substituent. With respect to acceptor groups, oxazines bearing donor groups are characterized not only by larger β_{HRS} and β_{HRS} contrast ratios but also by smaller excitation energies, larger opening-induced charge transfer, and reduction of the bond length alternation, as well as smaller Gibbs energies of the opening reaction. Compared to protonated open forms ($\mathbf{b}^+$), calculations on the zwitterionic open forms (**b**) have pointed out similarities in the long-wavelength UV/vis absorption spectra, whereas their β_{HRS} values might differ strongly as a function of the substituent. Indeed, the open forms present two NLOphores, the indoleninium-substituent entity and the nitrophenol (present in the protonated open form, $\mathbf{b}^+$) or nitrophenolate (present in the zwitterionic open form, **b**) moiety. Then, nitrophenolate displays a larger first hyperpolarizability than nitrophenol and the β tensor of the two entities might reinforce or cancel each other.

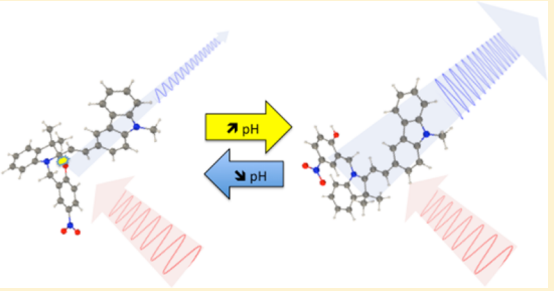

1. INTRODUCTION

Several families of molecules can exhibit structural changes in response to external stimuli. Such dynamical systems offer advantages because selected properties can reversibly be turned "on" and "off", with ensuing exploitations in devices such as sensors, actuators, or memories as well as in imaging.[1] The switching events can be triggered in many ways, including by irradiation at specific frequencies as well as by changing the pH, the temperature, or the redox potential. When these produce a spectral change, typically, but not necessarily, of visible color, these compounds are referred to as photochromes, acidochromes or halochromes, thermochromes, and electrochromes, respectively. Besides modifications of the linear optical properties (absorption and emission of light), of the reactivity, or of the complexation behavior, the stimuli can also trigger a variation of the nonlinear optical (NLO) properties such as second-harmonic generation (SHG), two-photon absorption (TPA), and third-harmonic generation (THG).[2] These compounds are known as NLO switches, opening the way toward multiaddressable, multistate, and multifunctional compounds. Still, a majority of them show a contrast of the first hyperpolarizability (β), the molecular property at the origin of SHG, rather than of higher-order responses.[3] To achieve large contrasts, one or several forms has to present a large NLO response. Molecules exhibiting large β are generally built from donor−π−acceptor (D−π−A) moieties, organized in noncentrosymmetric patterns. Linear NLOphores contain a unique D−π−A moiety, Λ-shape NLOphores contain two D−π−A units, sharing the same A or D group, and octupolar NLOphores contain three or four units, giving rise to C_{3h}- or T_d-like structures. Many studies have addressed the interplay between the D/A strength, the nature and length of the π-conjugated linker, and the first as well as second hyperpolarizabilities.[4] Based on these structure−property relationships, efficient NLO switching mechanisms consist, upon starting from a large-β form, in reducing the acceptor character of A, in reducing the donor character of D, or in breaking the π-conjugation between the D and A, any of these leading to a strong reduction of β. So far, many D−π−A compounds have

Received: December 18, 2015
Published: March 20, 2016

DOI: 10.1021/jacs.5b13243
J. Am. Chem. Soc. 2016, 138, 5052−5062

Scheme 1. Reference Indolinooxazolidine (1a) and Spiropyran (2a) NLO Switches Together with the Equilibria with Their Open Forms, As Triggered by Acid/Base Addition ($1b^+/2b^+$) or by Irradiation (1b/2b)

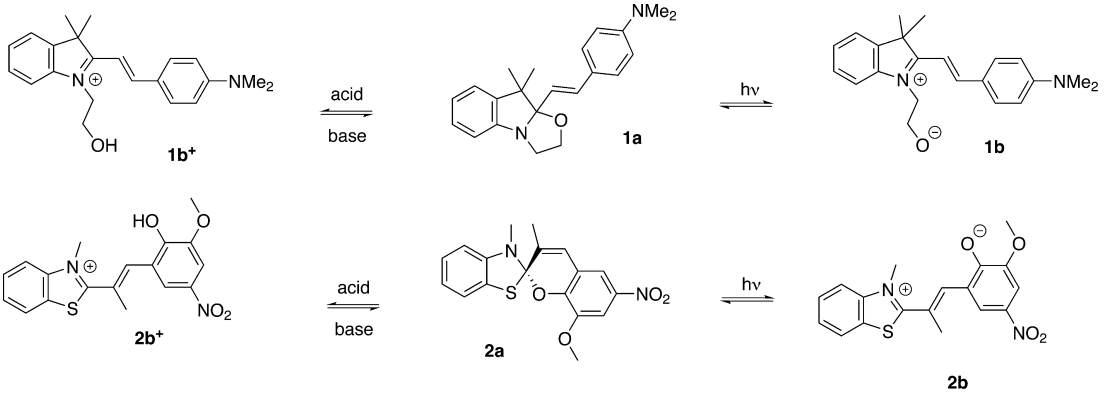

Scheme 2. Oxazines (3−12) in Their Closed (a), Zwitterionic Open (b), and Protonated Open (b^+) Forms

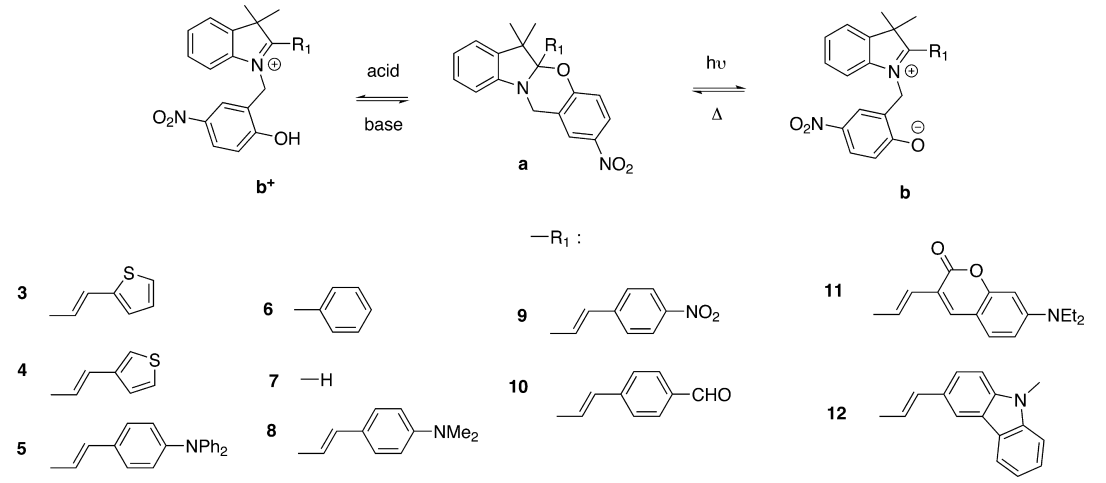

been shown to exhibit β contrasts, including azobenzenes,[5] diarylethenes,[6] nitrobenzylpyridines,[7] *N*-salicylidene-aniline,[8] organometallic complexes with Ru, Fe, Zn, and Pt transition metal atoms,[9] azafulleroids,[10] benzazolooxazolidines,[11] dithiazolylethenes,[12] spiropyrans,[13] dihydroazulene-vinylheptafulvene,[14] dicyanoimidazole,[15] styrilpyridines,[16] flavylium,[17] and quinolinium[18] ions as well as fluorescent proteins.[19] Among them, indolinooxazolidine[11] and spiropyran[13] derivatives were demonstrated to behave as highly efficient NLO switches, exhibiting large contrasts of first hyperpolarizability, and two of their representatives are used as reference compounds in this study (Scheme 1).

In this paper, the NLO switching performances of [1,3]-benzoxazine derivatives are revealed by means of a joint experimental−theoretical investigation. Several of these molecules, which fuse 2*H*,3*H*-indole and 2*H*,4*H*-benzo[1,3]oxazine heterocycles, have recently been synthesized by one of the authors and his collaborators[20] as well as by Zhu et al.[21] Based on their structural similarity with indolinooxazolidine and their switching optical properties, these compounds are expected to exhibit significant β contrasts. However, their structural differences with the later systems call for a detailed investigation of their NLO switching properties. Indeed, it was already observed that oxazines can undergo three types of opening mechanism by cleavage of the C−O bond at the junction of the two heterocycles: photochemical, redox,[21] or induced by acidic addition.[20] This opening leads to the formation of a phenolate (photochemical and redox) or a phenol (pH) chromophoric moiety while it allows for π-conjugation between the R_1 substituent and the indoleninium unit (Scheme 2). Both **b** and $\mathbf{b}^+$ open forms exhibit considerable changes in their UV/vis absorption spectra compared to their associated closed form. The opening mechanisms have already been the subject of theoretical and experimental investigations.[22]

Based on refs 20−21, 10 oxazine derivatives were selected, with R_1 substituents covering a broad range of D/A character (Scheme 2). Note that three of these have not been synthesized so far (**7**, **9**, and **10**) while they constitute alternative substitution patterns. In a first step, together with the two reference compounds, the structural, electronic, thermodynamic, linear, and nonlinear optical properties of these oxazines were determined by employing quantum chemistry methods. The simulations allowed establishing structure−property relationships and design guidelines to enhance the β contrasts of this new family of NLO switches. From these, four compounds have been selected because they are representatives of oxazines having large (**11** and **12**) or intermediate (**3** and **4**) β_{HRS} responses in their open forms and because their β_{HRS} contrast ratios are clearly distinct from one. These compounds were then subjected to experimental characterizations of their nonlinear optical properties by means of hyper-Rayleigh scattering (HRS)[23] measurements as well as of their UV/vis absorption spectra while further interpretations were carried out using *ab initio* calculations. Only the closed and protonated

DOI: 10.1021/jacs.5b13243
J. Am. Chem. Soc. 2016, 138, 5052−5062

open forms were experimentally characterized, since the photogenerated species have too short lifetimes (μs). The paper is organized as follows. After describing the essentials of the experimental and quantum chemistry methods, we start by presenting the experimental results on the four selected compounds (**3**−**4** and **11**−**12**) and by interpreting these utilizing theoretical results. Then, the detailed theoretical investigations on the complete set of compounds are reported and discussed in terms of structure−property relationships, before conclusions are drawn.

2. METHODS

2.1. Synthesis and Preparation of the Solutions. Details about the synthesis of compounds **3**−**4** and **11**−**12** can be found in ref 20c. HRS measurements were performed with diluted solutions in chloroform with chromophore concentrations ranging from 10^{-3} to 10^{-4} M for **3a**, **4a**, and **12a**, from 5×10^{-4} to 5×10^{-5} M for **11a**, and from 10^{-4} to 10^{-5} for $\mathbf{3b}^+$, $\mathbf{4b}^+$, $\mathbf{11b}^+$, and $\mathbf{12b}^+$. All solutions were centrifuged during 20 min to prevent spurious scattering from particles.

2.2. Linear and Nonlinear Optical Property Characterizations. Following the methodology of Raymo et al.,[20] the closed forms were stabilized using small quantities of triethylamine (Et_3N) while the protonated open form was obtained by adding trifluoroacetic acid (TFA) in small excess (indeed, vapors of TFA failed to trigger the closed form). Note that the pK_a of the substituents of **11** and **12** are below the one of TFA (0.52), so they undergo no protonation during the opening process, as would have been evidenced, for **12**, by the appearance of a new band at *ca*. 430 nm. UV/vis absorption spectra were recorded on a PerkinElmer Lambda 650 spectrophotometer in chloroform.

The experimental procedure to gain the HRS quantities has been previously reported by Rodriguez and co-workers,[24] performed on diluted solutions with an incident radiation of 1064 nm. The HRS signal originates from individual scatterers without any phase relations between each other in solution. This signal, $I^{2\omega}$, is therefore related to the individual molecular first hyperpolarizability and can be expressed, for incoherent and uncorrelated scatterers, as

$$I^{2\omega} = G f_L^2 C \langle \beta_{HRS}^2 \rangle (I^{\omega})^2 \tag{1}$$

where I^{ω} is the incident intensity, $\langle \beta_{HRS}^2 \rangle$ is the orientational average of the first hyperpolarizability tensor over all possible molecular orientations, G is a constant containing the parameters of the experimental setup, C is the concentration of the solution, and f_L is a local field correction approximated using the high-frequency Lorentz−Lorenz spherical cavity expression (with refractive index of the liquid for both optical frequencies ω and 2ω). In the setup, a 90° angle is fixed between the directions of propagation of the incident and of the scattered SHG beams. The fundamental light beam is propagating in the Y-direction and analyzed in the X-direction (note that X, Y, and Z stand for the laboratory coordinates system, while the molecular coordinates are written as x, y, and z). Assuming these conditions, the impact of the incident light polarization on the intensity of the Z-polarized (vertical) scattered beam was derived by Bersohn et al.:[25]

$$I_{\Psi V}^{2\omega} \propto \langle \beta_{ZXX}^2 \rangle \cos^4 \Psi + \langle \beta_{ZZZ}^2 \rangle \sin^4 \Psi + \sin^2 \Psi \cos^2 \Psi \langle (\beta_{ZXZ} + \beta_{ZZX})^2 + 2\beta_{ZZZ}\beta_{ZXX} \cos 2\delta \rangle \tag{2}$$

where Ψ and δ characterize the state of polarization of a general elliptically polarized incident light. The experimental setup contains a quarter-wave plate ($\lambda/4$, which converts linearly polarized light into left/right elliptical, circular polarized light) after a rotatable half-wave plate ($\lambda/2$, which rotates the plane of linear polarization), providing a phase retardation of $\delta = \pi/2$ and allowing the change of polarization from vertical (V, parallel to Z, $\Psi = \pi/2$) to horizontal (H, parallel to X, $\Psi = 0$) via left and right circular polarization ($\pm\pi/4$) and elliptic polarization (although all values of Ψ can be obtained). The relationships between the orientationnal averages (in the laboratory frame) and the molecular tensor components (in the molecular frame) read as follows:

$$\begin{aligned}\langle \beta_{ZZZ}^2 \rangle = {} & \frac{1}{7}\sum_{\zeta}^{x,y,z} \beta_{\zeta\zeta\zeta}^2 + \frac{4}{35}\sum_{\zeta\neq\eta}^{x,y,z} \beta_{\zeta\zeta\eta}^2 + \frac{2}{35}\sum_{\zeta\neq\eta}^{x,y,z} \beta_{\zeta\zeta\zeta}\beta_{\zeta\eta\eta} \\ & + \frac{4}{35}\sum_{\zeta\neq\eta}^{x,y,z} \beta_{\eta\zeta\zeta}\beta_{\zeta\zeta\eta} + \frac{4}{35}\sum_{\zeta\neq\eta}^{x,y,z} \beta_{\zeta\zeta\zeta}\beta_{\eta\eta\zeta} + \frac{1}{35}\sum_{\zeta\neq\eta}^{x,y,z} \beta_{\eta\zeta\zeta}^2 \\ & + \frac{4}{105}\sum_{\zeta\neq\eta\neq\xi}^{x,y,z} \beta_{\zeta\zeta\eta}\beta_{\eta\xi\xi} + \frac{1}{105}\sum_{\zeta\neq\eta\neq\xi}^{x,y,z} \beta_{\eta\zeta\zeta}\beta_{\eta\xi\xi} \\ & + \frac{4}{105}\sum_{\zeta\neq\eta\neq\xi}^{x,y,z} \beta_{\zeta\zeta\eta}\beta_{\xi\xi\eta} + \frac{2}{105}\sum_{\zeta\neq\eta\neq\xi}^{x,y,z} \beta_{\zeta\eta\xi}^2 \\ & + \frac{4}{105}\sum_{\zeta\neq\eta\neq\xi}^{x,y,z} \beta_{\zeta\eta\xi}\beta_{\eta\zeta\xi}\end{aligned} \tag{3}$$

$$\begin{aligned}\langle \beta_{ZXX}^2 \rangle = {} & \frac{1}{35}\sum_{\zeta}^{x,y,z} \beta_{\zeta\zeta\zeta}^2 + \frac{4}{105}\sum_{\zeta\neq\eta}^{x,y,z} \beta_{\zeta\zeta\zeta}\beta_{\zeta\eta\eta} - \frac{2}{35}\sum_{\zeta\neq\eta}^{x,y,z} \beta_{\zeta\zeta\zeta}\beta_{\eta\eta\zeta} \\ & + \frac{8}{105}\sum_{\zeta\neq\eta}^{x,y,z} \beta_{\zeta\zeta\eta}^2 + \frac{3}{35}\sum_{\zeta\neq\eta}^{x,y,z} \beta_{\zeta\eta\eta}^2 - \frac{2}{35}\sum_{\zeta\neq\eta}^{x,y,z} \beta_{\zeta\zeta\eta}\beta_{\eta\zeta\zeta} \\ & + \frac{1}{35}\sum_{\zeta\neq\eta\neq\xi}^{x,y,z} \beta_{\zeta\eta\eta}\beta_{\zeta\xi\xi} - \frac{2}{105}\sum_{\zeta\neq\eta\neq\xi}^{x,y,z} \beta_{\zeta\zeta\xi}\beta_{\eta\eta\xi} \\ & - \frac{2}{105}\sum_{\zeta\neq\eta\neq\xi}^{x,y,z} \beta_{\zeta\zeta\eta}\beta_{\eta\xi\xi} + \frac{2}{35}\sum_{\zeta\neq\eta\neq\xi}^{x,y,z} \beta_{\zeta\eta\xi}^2 \\ & - \frac{2}{105}\sum_{\zeta\neq\eta\neq\xi}^{x,y,z} \beta_{\zeta\eta\xi}\beta_{\eta\zeta\xi}\end{aligned} \tag{4}$$

Note that these expressions are simplified if Kleinman's conditions are used. Since for nonpolarized/natural incident light both H and V polarizations have equal weights, the orientational average is the sum of the two previous equations, determining therefore the full HRS response, as

$$\beta_{HRS} = \sqrt{\langle \beta_{HRS}^2 \rangle} = \sqrt{\langle \beta_{ZZZ}^2 \rangle + \langle \beta_{ZXX}^2 \rangle} \tag{5}$$

The associated depolarization ratio (DR), which gives information on the geometry of the NLOphore, i.e. the part of the molecule responsible for the NLO response, reads as follows:

$$DR = \frac{I_{VV}^{2\omega}}{I_{HV}^{2\omega}} = \frac{\langle \beta_{ZZZ}^2 \rangle}{\langle \beta_{ZXX}^2 \rangle} \tag{6}$$

β is also typically decomposed into the sum of dipolar ($J = 1$) and octupolar ($J = 3$) tensorial components. Assuming Kleinman's conditions,

$$\langle \beta_{ZZZ}^2 \rangle = \frac{9}{45}|\beta_{J=1}|^2 + \frac{6}{105}|\beta_{J=3}|^2 \tag{7}$$

$$\langle \beta_{ZXX}^2 \rangle = \frac{1}{45}|\beta_{J=1}|^2 + \frac{4}{105}|\beta_{J=3}|^2 \tag{8}$$

The nonlinear anisotropy parameter $\rho = |\beta_{J=3}|/|\beta_{J=1}|$ compares the relative contributions of the octupolar and dipolar components to the first hyperpolarizability tensor β while it is linked to the depolarization ratio:

$$DR = 9\frac{\left(1 + \frac{2}{7}\rho^2\right)}{\left(1 + \frac{12}{7}\rho^2\right)} \tag{9}$$

Finally, using these expressions, β_{HRS} can be rewritten under the following form:

DOI: 10.1021/jacs.5b13243
J. Am. Chem. Soc. 2016, 138, 5052−5062

$$\beta_{HRS} = \sqrt{\frac{10}{45}|\beta_{J=1}|^2 + \frac{10}{105}|\beta_{J=3}|^2} = |\beta_{J=1}|\sqrt{\frac{2}{3}\left(\frac{1}{3} + \frac{1}{7}\rho^2\right)} \quad (10)$$

For a solution of two components (solute and solvent) where both give rise to a β response, $I^{2\omega}$ originates from both and is given by

$$I^{2\omega}_{\Psi V} = Gf_L^2\{C_S|\beta_{J=1}|^2_S C^S_{\Psi V} + C_X|\beta_{J=1}|^2_X C^X_{\Psi V}\}10^{-\varepsilon^{2\omega}_X dC_X}(I^{\omega})^2 \quad (11)$$

where the subscripts S and X stand for the solvent and the chromophore, respectively. $\varepsilon^{2\omega}_X$ accounts for the one-photon absorption of the chromophore at the second harmonic frequency, d is the optical path of the scattered harmonic light, and $C_{\Psi V}$ is the orientational average of the spherical components of the molecular first hyperpolarizability, given by

$$C_{\Psi V} = \left\{\left(\frac{9}{45} + \frac{6}{105}\rho^2\right) + \left(-\frac{20}{45} + \frac{10}{105}\rho^2\right)\cos^2\Psi + \left(\frac{12}{45} - \frac{12}{105}\rho^2\right)\cos^4\Psi\right\} \quad (12)$$

In the current procedure, the determination of β_{HRS} goes through the evaluation of $|\beta_{J=1}|$ and ρ for each compound. $|\beta_{J=1}|^2$ C^X_{VV} is then obtained via eq 11 by varying the incident intensity I^{ω} for different concentrations, with vertical (V) incident polarization ($\Psi = \pi/2$). Following ref 24a, the values for chloroform, used as solvent and internal reference, are $|\beta_{J=1}|_S$ = 25.3 au and ρ_S = 1.836 at 1064 nm, giving thus C^S_{VV} = 0.393. Taking C_S = 12.47 mol L^{-1}, it gives $C_S|\beta_{J=1}|^2_S$ C^S_{VV} = 3140 mol L^{-1} (a.u.)^2. Then, the anisotropy factor of the chromophore, ρ_X, is evaluated by polarization scan of the scattered light with a constant incident power for both the solvent and the chromophore solution at a given concentration. This allows determining C^X_{VV} and then $|\beta_{J=1}|_X$. Finally, β_{HRS} and DR are evaluated using eqs 10 and 9, respectively.

HRS measurements were performed with diluted solutions (ranging from 10^{-3} M to 5×10^{-5} M) in chloroform. The incident radiation at 1064 nm is obtained from a Nd:YVO_4 laser that produces trains of about 65 ps, $\leq$ 50 μJ pulses at a repetition rate of 2 kHz (PL2200 Laser, EKSPLA). The polarized incident laser beam is focused into the sample cell with a 5X Mitutoyo Plan APO NIR objective (infinity-corrected with NA = 0.14) and positioned to pass at a distance of ~1−2 mm from the inside of the cell wall facing the collecting lens. The incident laser beam waist has a diameter of approximately 10 μm with a Rayleigh range of about 200 μm. The scattered light at the double frequency (532 nm) is collected at 90° with f/1.2 optics and focused into a modified Horiba spectrograph, with vertical (V) polarization selection. The entrance slits of the spectrograph are closed to fit the full beam waist image. The spectrally dispersed light (using an 1800 grooves per mm grating), detected by a nitrogen-cooled CCD camera (2048 × 512 pixels) in a continuous acquisition mode, is collected around the 532 nm harmonic light scattering and covered a spectral range of about 1800 cm^{-1} with a spectral slit width of about 15 cm^{-1}. The spatial resolution is estimated using the CCD image mode, and in any case, the HRS signal is confined to dimensions less than the Rayleigh range so that no correction for the effect of a finite collection angle is required. Typical acquisition times to achieve good signal-to-noise spectra are 3 × 20 s. The hyper-Rayleigh intensity is obtained by integrating the signal from −200 to +200 cm^{-1} after eliminating the background, which was extrapolated by a linear law obtained by excluding this spectral range.[17]

Since the measurements are performed at 1064 nm, the β_{HRS} responses of some chromophores are impacted by electronic resonance, which prevents comparisons between equivalent compounds. Therefore, the 1064 nm values have been extrapolated to 1907 nm by using the homogeneously damped two-level model,[26] which is an approximation to the sum-over-states expression of β.[27] This method accounts for the relative position of the incident and SHG photon energies with respect to the position of the UV/vis absorption band maximum as well as for the width of the absorption band.

2.3. Quantum Chemical Calculations. All geometry optimizations were carried out at the density functional theory (DFT) level using the M06 exchange correlation (XC) functional[28] and the 6-311G(d) basis set. This XC functional contains 27% of Hartree−Fock exchange. For all compounds and forms, a search for the most stable geometries was carried out by sampling the conformational space. This was achieved by considering several starting geometries, differing mostly by the values of the torsion angles around the single bonds. A detailed conformational investigation was carried out for **3b**$^+$ to confirm that the most stable conformer is sufficient to provide an accurate estimate of β of a given compound/form. In that case, 9 minima were located on the potential energy surface within an energy range of 50 kJ/mol and their β_{HRS} responses were calculated at the IEF-PCM(chloroform)/TDHF/6-311+G(d) level (*vide infra*). Using the Maxwell−Boltzmann expression, the average value amounts to 3373 au, which only differs by 0.3% from the value of the most stable conformer, which substantiates the use of the "one conformer" approach. For all compounds and forms the optimized structures are characterized by 3*N*-6 real vibrational frequencies (with *N* as the number of atoms). The latter were subsequently used in a thermochemistry analysis (T = 298.15 K, P = 1 atm), where the standard enthalpy (H°), entropy (S°), and Gibbs free energy (G°) are calculated in order to characterize the cleavage reactions.

Excitation energies ($\Delta E = h\upsilon = hc/\lambda$) and corresponding oscillator strengths (f) of the dominant low-energy electronic transitions were calculated at the time-dependent DFT (TDDFT) level with the M06-2X[28] XC functional together with the 6-311+G(d) basis set. The M06-2X XC functional has been selected owing to its good performance for calculating the excitation energies of the closed and open forms of oxazine, of which the excitations present small- and medium-range charge transfer character,[29] in agreement with recent investigations on NLOphores[4f] whereas M06 is a general-purpose XC functional for geometry optimization.[28]

The first hyperpolarizabilities were evaluated at several levels of approximation, i.e. with the time-dependent Hartree−Fock (TDHF) method[30] to gain the dynamic responses, with the coupled-perturbed Hartree−Fock (CPHF) scheme to obtain their static equivalents, and with the second-order Møller−Plesset perturbation theory (MP2) approach to account for electron correlation effects. Several investigations on push−pull π-conjugated systems have indeed shown that the largest part of electron correlation effects is included at the MP2 level.[31] The MP2 values were calculated using the finite field (FF) procedure[32] implying a Romberg scheme to improve the accuracy on the numerical derivatives.[33] This is now performed by following an automatic procedure described in ref 33b. The numerical accuracy on these third-order derivatives of the energy (the opposite of which gives the β tensor components) attains typically 0.5 au or better, compared to analytical calculations performed at the same level of approximation. To account for frequency dispersion and electron correlation simultaneously, the multiplicative scheme was applied.[33b,34] It consists of multiplying the static FF/MP2 values by the ratio between the TDHF and CPHF responses:

$$\beta_{MP2}(-2\omega;\omega,\omega) \approx \beta_{MP2}(0;0,0) \times \frac{\beta_{TDHF}(-2\omega;\omega,\omega)}{\beta_{CPHF}(0;0,0)} \quad (13)$$

All reported β values are given in au [1 au of β = 3.6213 × 10^{-42} m^4 V^{-1} = 3.2064 × 10^{-53} C^3 m^3 J^{-2} = 8.639 × 10^{-33} esu] within the T convention.[35]

Solvent effects were consistently included in all the calculations (geometry optimizations, thermochemistry, linear and nonlinear optical property calculations) using the polarizable continuum model within the integral equation formalism (IEF-PCM).[36] In this model, the solute is placed in a cavity defined by interlocking spheres centered on the nuclei with atomic van der Waals radii from the Universal Force Field, this cavity being in a structureless continuum, characterized by a dielectric constant, ε. The solute−solvent interactions are described by

DOI: 10.1021/jacs.5b13243
J. Am. Chem. Soc. 2016, 138, 5052−5062

surface charges located on the outer surface of the cavity, adjusted iteratively according the electron density of the solute. Two solvents were used, following those employed in the experimental characterizations, i.e. (i) chloroform, employed in the measurements reported here (ε_0 = 4.711 and ε_∞ = 2.091), and (ii) acetonitrile (ε_0 = 35.688 and ε_∞ = 1.807) employed in ref 20 for the photochemical studies. Both static (ε_0) and infinite-frequency (ε_∞) dielectric values are necessary to determine the dynamic dielectric constant at any frequency (ε_ω), using the relationship $\varepsilon_\omega = \varepsilon_\infty + (\varepsilon_0 - \varepsilon_\infty)/(1 - i\omega\tau_D)$, where $\tau_D = 0.85 \times 10^{-11}$ s is a characteristic time associated with the solvent reorganization. All the calculations were performed using the Gaussian09 package.[37]

3. RESULTS AND DISCUSSION

3.1. Experimental and Theoretical Studies of Compounds 3−4 and 11−12. The UV/vis absorption spectra were recorded in chloroform solutions for the closed and protonated open forms of compounds **3**, **4**, **11**, and **12**. They are presented in Figure S1 while the maximum absorption wavelengths (λ^{max}) of the lowest-energy transitions are listed in Table 1 together with the vertical transition wavelengths (λ^{vert})

Table 1. UV/vis Absorption Spectra of Closed and Protonated Open Forms of 3, 4, 11, and 12: Experimental Maximum Absorption Wavelengths (nm), Energies (eV), and Extinction Coefficients (10^3 M^{-1} cm^{-1}) As Well As Vertical Transition Wavelengths (nm), Energies (eV), and Associated Oscillator Strengths Calculated at the TDDFT/M06-2X Level

	expt λ^{max}, ΔE^{max} (ε)	calcd λ^{vert}, ΔE^{vert} (f)
3a	292, 4.25 (7.8)	273, 4.54 (0.680)
3b$^+$	446, 2.78 (23.4)	418, 2.96 (1.064)
4a	318, 3.90 (11.6)	280, 4.42 (0.480)
4b$^+$	421, 2.94 (26.0)	393, 3.15 (1.000)
11a	408, 3.04 (11.5)	359, 3.46 (1.317)
11b$^+$	610, 2.03 (21.5)	493, 2.52 (1.990)
12a	289, 4.29 (21.6)	266, 4.66 (0.990)
12b$^+$	545, 2.27 (31.2)	456, 2.72 (1.453)

and associated oscillator strengths (f) calculated at the IEP-PCM(chloroform)/TDDFT/M06-2X/6-311+G(d) level of approximation. Both experiment and calculations display the same trends: (i) opening the oxazine leads to a large reduction of the excitation energy, from 0.96 eV for **4** to 2.02 eV for **12**; (ii) the ordering of the absorption wavelengths changes between the closed (**12a** < **3a** < **4a** < **11a**) and open (**4b**$^+$ < **3b**$^+$ < **12b**$^+$ < **11b**$^+$) form, evidencing the effects of the increase of the π-conjugated path upon C−O cleavage (*vide infra*).

The calculated vertical excitation energies (wavelengths) are systematically larger (smaller) than the experimental maximum absorption values, but the experimental changes between compounds are well reproduced by the calculations carried out at the TDDFT/M06-2X level. So, the slope of the TDDFT versus experimental least-squares linear regression relationship is close to 1 as well as the R^2 correlation coefficient (Table S1). In addition to the low-energy peak (450−610 nm), the protonated open forms also present a second and less-intense absorption that peaks near 320 nm. It is attributed to the electronic excitation of the nitrophenol moiety. This spectral feature is also reproduced by the TDDFT calculations.

The β_{HRS} and DR were determined for both forms in chloroform (Table 2), leading to contrast ratios ranging from

Table 2. β_{HRS} (au) and DR of Closed and Protonated-Open Forms of Compounds 3−4 and 11−12 As Determined Experimentally in Chloroform (λ = 1064 nm) As Well As Their β_{HRS}(open)/β_{HRS}(closed) Ratios

	closed (a)		open (b$^+$)		
	β_{HRS}	DR	β_{HRS}	DR	open/closed β_{HRS} ratio
3	1910	4.33	4820	4.76	2.45
4	2050	5.12	4480	5.17	2.18
11	5210	6.75	52 820	4.94	10.1
12	1970	4.06	54 530	5.03	27.7

2.2 to 28. The corresponding power scans and polarization scans are given in Figures S2−S5. As expected, the acido-triggered oxazine opening gives rise to a π-conjugated segment linking the indoleninium acceptor group with moieties exhibiting various donor characters, inducing a large increase of the first hyperpolarizability. All DRs are close to 5, the typical value of one-dimensional push−pull π-conjugated systems, and this is even more obvious in the case of open forms. Nevertheless, the discussion on the relative β_{HRS} and contrast amplitudes is not straightforward because it is impacted by resonance, in particular in the case of compound **12b**$^+$ that presents a maximum absorption at 545 nm whereas the 532 nm SHG wavelength is within the absorption band. Note that for **11a** there are possible perturbations from additional forms that hamper a good evaluation of the response of that closed form (see polarization scan, Figure S4). As a consequence, the amplitude of the β_{HRS} response reported in Table 2 is likely underestimated, while the DR value is likely overestimated. Solvent effects (chloroform) or impurities on the coumarin part are probably at the origin of these perturbations, as indicated by variations of ρ as a function of concentration (not shown). To allow more reliable comparisons between the intrinsic NLO properties of the compounds, the β_{HRS} values measured at 1064 nm were extrapolated to 1907 nm, i.e. far from resonance, by using the homogeneously damped two-level model (*vide supra*). Since the absorption bandwidth changes from one compound/form to another, the damping factor (Γ) was determined by least-squares fitting a Gaussian function to the absorption band. The Γ values are listed in Table S2, together with the frequency dispersion factors F defined as $F = \beta_{HRS}(1064)/\beta_{HRS}(1907)$. Γ is systematically larger for the compounds with a thiophene moiety and decreases upon C−O cleavage. Combining these relative values with the excitation energies gives dispersion factors of ∼1.35 for **3a**, **4a**, and **12a** and of ∼2.0 for **11a**, **3b**$^+$, **4b**$^+$, and **11b**$^+$, whereas F gets larger for **12b**$^+$ (3.05). This reflects on the β_{HRS}(open)/β_{HRS}(closed) contrasts at 1907 nm, which become smaller for compounds **3**, **4**, and **12** but remain unchanged for compound **11**. Still, the contrasts are clearly sufficient to evidence the acido-triggered switching (Table 3).

Ab initio calculations of β_{HRS} were used to rationalize these data. In these calculations, electron correlation was included at the MP2 level, frequency dispersion was approximated using the multiplicative scheme (eq 13), and solvent (chloroform) effects were accounted for within IEF-PCM (*vide supra*). The intermediate quantities to evaluate β_{HRS}^{MP2} (1907) are listed in Table S3, substantiating once again that electron correlation effects as determined at the MP2 level typically account for an increase of β_{HRS} by a factor of 2 or more compared to

DOI: 10.1021/jacs.5b13243
J. Am. Chem. Soc. 2016, 138, 5052−5062

Table 3. Experiment (Extrapolated) versus Theoretical β_{HRS} of the Closed and Protonated-Open Forms of Compounds 3−4 and 11−12 As Well As Their $\beta_{HRS}(b^+)/\beta_{HRS}(a)$ Ratios[a]

	Experiment			Calculations		
	Closed (**a**)	Open ($\mathbf{b}^+$)	$\beta_{HRS}(b^+)/\beta_{HRS}(a)$	Closed (**a**)	Open ($\mathbf{b}^+$)	$\beta_{HRS}(b^+)/\beta_{HRS}(a)$
3	1410	2330	1.65	1308	4734	3.62
4	1520	2240	1.47	1283	3939	3.07
11	2600	26 400	10.1	6416	31 588	4.92
12	1460	17 880	12.2	2092	17 257	8.25

[a]All values correspond to a 1907 nm wavelength, far from resonance, which enables estimation of the intrinsic molecular responses and comparison of calculations with experiments.

uncorrelated HF calculations. The final *ab initio* values as well as the contrast ratios are given in Table 3 with the experimental values, while the close relationship between experiment and calculations is highlighted in Figure 1. The main observations

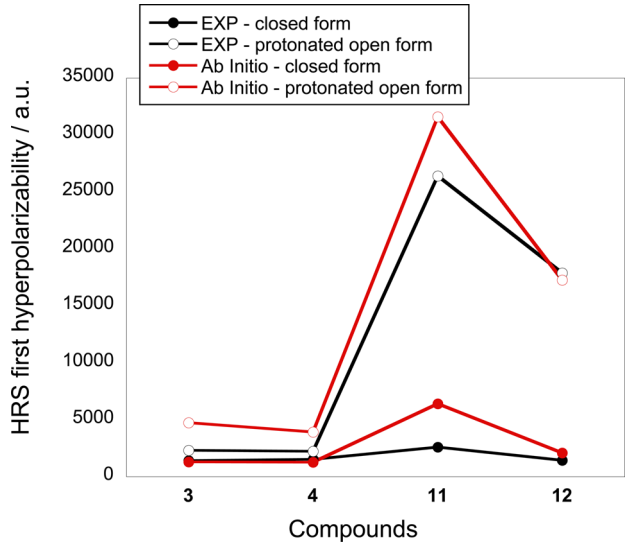

Figure 1. Experimental versus *ab initio* β_{HRS} values (λ = 1907 nm).

are as follows: (i) the open forms have larger β_{HRS} values than the closed forms; (ii) compounds **11** and **12** have larger β_{HRS} values—and β_{HRS} contrasts—especially in their open forms than compounds **3** and **4**; (iii) compound $\mathbf{11b}^+$ possesses the largest β_{HRS} response but the largest contrast ratio is associated with compound **12**. Besides, there are some differences between the two sets of results. In particular, the calculated β_{HRS} responses are noticeably larger than the measured ones for **11a**, $\mathbf{3b}^+$, and $\mathbf{4b}^+$. This might originate from the approximations used in the calculations, in particular the description of frequency dispersion, as well as in the treatment of the experimental data when extrapolating the β_{HRS} response from 1064 to 1907 nm. For **11a**, as mentioned above, it is also possible that the measured β_{HRS} is underestimated.

3.2. Theoretical Study of Oxazines 3−12 in Comparison to Reference Systems 1−2. The geometries of the closed and (zwitterionic and protonated) open forms of **1**−**12** in their electronic ground state were optimized at the M06/6-311G(d) level of approximation with the IEF-PCM approach (solvent = chloroform). For oxazines, when the R_1 substituent contains a vinylene linker, the bond length alternation [BLA = $(d_1 - 2d_2 + d_3)/2$) along this latter was evaluated (Table 4), highlighting the relationship with the D/A nature of the terminal group R_1'. Indeed, in the open form, the double bond is in resonance with the indoleninium function, which leads to a substantial reduction of BLA from 0.14 ± 0.01 Å to 0.05 ± 0.03 Å. In particular, owing to the acceptor character of the indoleninium, the smallest BLA values are obtained when R_1' is a donor group (compounds **5** and **8** as well as **11** and **12**) whereas the largest are obtained with acceptor groups (compounds **9** and **10**). We also note that the BLA values of the protonated $\mathbf{b}^+$ forms are overall smaller than those of the phototriggered open forms, which is attributed to stronger electrostatic effects in the zwitterionic forms.

For both opening reactions, the Gibbs energies (T = 298.15 K, P = 1 atm) were evaluated at the IEF-PCM(chloroform)/M06/6-311G(d) level of approximation (Table 5). These reactions are endergonic, and ΔG^θ is smaller for small donor substituents (**5**, **8**) than for acceptor ones (**9**, **10**) or large donor ones (**11**, **12**). The largest ΔG^θ values are obtained for the smallest substituents, without a vinylic linker (**6**, **7**).

The Mulliken, Hirshfeld, and Natural Population charge analyses, carried out by considering six molecular moieties (S_1−S_5 and R_1) (Figure 2, Table S4, and Figure S6a−c), describe consistently the redistribution of the charge upon opening. For the closed forms, the nitrophenol moiety (S_5) is electron-rich, which is attributed to the nitro acceptor group. The nitrogen (S_3) is strongly negative, owing to its large electronegativity. In contrast, the benzene ring (S_1), the carbon bearing the substituent (S_4), and the substituent (R_1) are positively charged. The phototriggered opening leads mainly to electron transfer from the benzene ring (S_1), the C=N group ($S_3 + S_4$), and the substituent (R_1) to the nitrophenol (S_5). This results

Table 4. M06/6-311G(d) Optimized BLA = $(d_1 - 2d_2 + d_3)/2$ (Å) for Compounds 3−5 and 8−12 As Obtained from Geometry Optimizations within IEFPCM (Solvent = Chloroform)

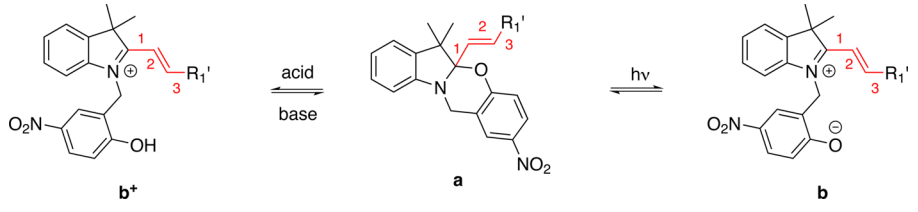

	3	4	5	8	9	10	11	12
closed (**a**)	0.136	0.140	0.142	0.139	0.146	0.145	0.136	0.143
open (**b**)	0.052	0.063	0.048	0.040	0.085	0.081	0.053	0.055
open ($\mathbf{b}^+$)	0.044	0.061	0.030	0.025	0.083	0.075	0.034	0.042

DOI: 10.1021/jacs.5b13243
J. Am. Chem. Soc. 2016, 138, 5052−5062

Table 5. M06/6-311G(d) ΔG^{θ} of the Opening Reactions (kJ mol^{-1}) and ΔS^{θ} (J mol^{-1} K^{-1}) in Parentheses[a]

	a ⇌ b	a + CF_3COOH ⇌ b^+ + CF_3COO^-
1	152.5 (11.5)	63.8 (13.9)
2	32.9 (46.9)	106.8 (11.0)
3	38.0 (18.0)	126.4 (14.4)
4	26.9 (31.6)	104.5 (19.8)
5	22.0 (23.7)	97.5 (30.1)
6	60.1 (42.8)	125.2 (35.0)
7	76.7 (25.3)	150.3 (10.3)
8	13.1 (16.5)	89.7 (24.5)
9	41.6 (24.6)	123.4 (23.6)
10	44.2 (12.1)	137.2 (13.2)
11	44.4 (19.0)	98.8 (18.4)
12	37.0 (25.3)	83.4 (23.3)

[a]Solvent (chloroform) effects were accounted for using the IEF-PCM model.

from the fact that opening the oxazine involves the formation of a phenolate and the appearance of a polar C=N$^+$ group π-conjugated with R_1. The S_2 group plays the role of spectator and is almost unaffected by the ring opening. Specific behaviors are observed (i) for compounds **6** and **7**, for which S_3 becomes slightly less negative, and (ii) for compounds **5**, **8**, **11**, and **12**, of which the donor R_1 moiety gets more positive, whereas (iii) the charge on the acceptor group R_1 of compounds **9** and **10** hardly changes. Besides S_5 bearing the proton, similar charge variations are observed upon acido-triggered opening. Indeed, from comparison of forms **b** and **b**$^+$ (Figure S6), about 90% of the proton charge is located on the nitrophenol moiety whereas the remainder of the excess charge goes to R_1 (with the exception of compounds **6** and **7**, where there is no π-conjugation between R_1 and the rest of the molecule).

The TDDFT/M06-2X vertical excitation energies of the dominant low-energy dipole-allowed excited state of compounds **1**−**12** are listed in Table 6, together with their oscillator

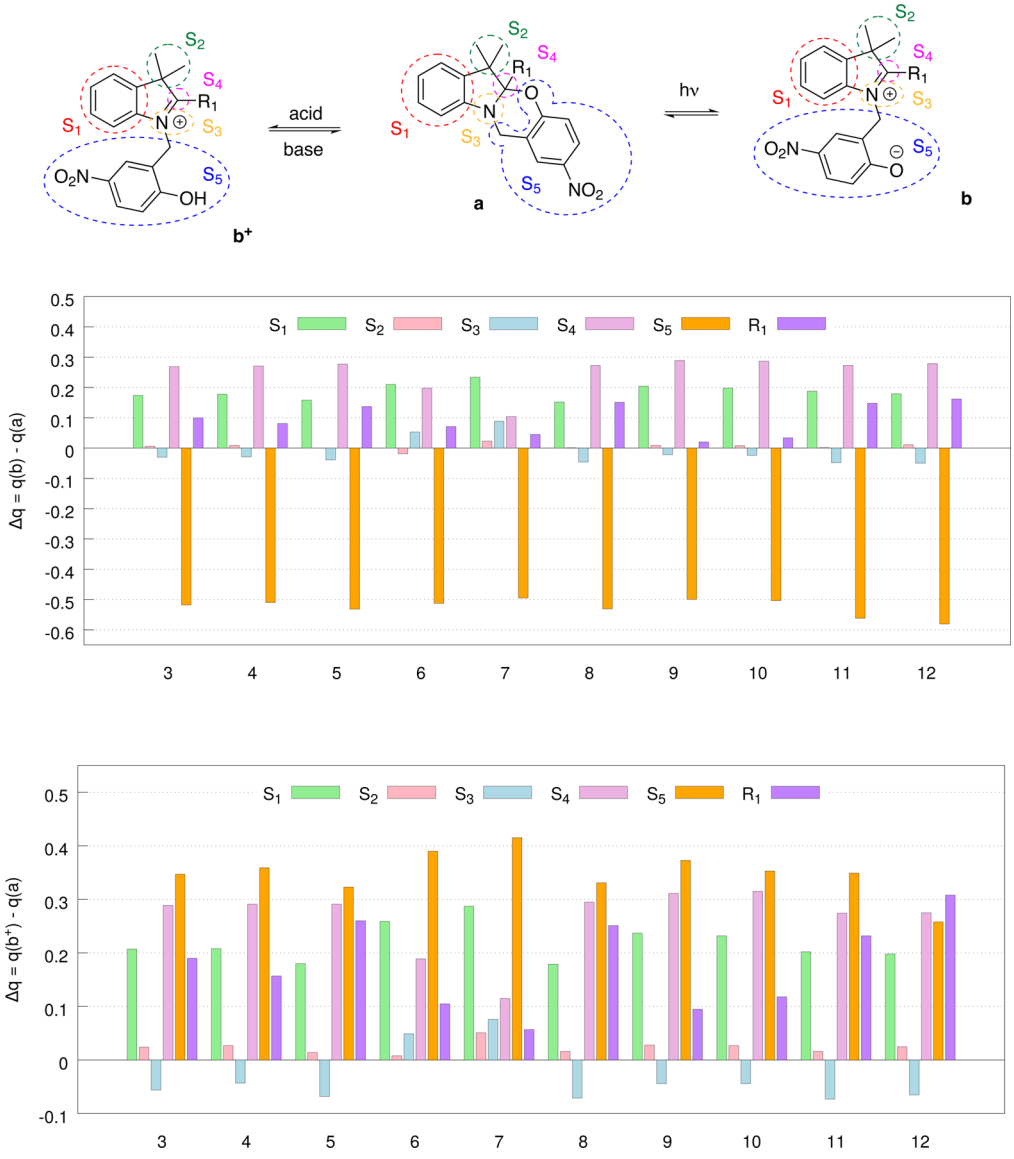

Figure 2. Spatial distribution on the S_1−S_5 and R_1 molecular moieties of the variations of the Mulliken charges when opening the oxazine, as determined at the IEF-PCM/M06/6-311G(d) level (in chloroform). (Top) Phototriggered opening, $\Delta q = q(\mathbf{b}) - q(\mathbf{a})$; (Bottom) acido-triggered opening, $\Delta q = q(\mathbf{b}^+) - q(\mathbf{a})$.

DOI: 10.1021/jacs.5b13243
J. Am. Chem. Soc. 2016, 138, 5052−5062

Table 6. Vertical Excitation Energies (ΔE^{vert}, eV), Oscillator Strengths (f, in Parentheses), and Main Character of the Dominant Low-Energy Dipole-Allowed Excited States of Compounds 1−12 in Their Closed and Open Forms, As Obtained at the IEF-PCM/TDDFT/M06-2X/6-311+G(d) Level of Approximation (in Chloroform)[a]

	closed (**a**)		open (**b**)		open (**b**$^+$)	
	ΔE^{vert} (f)	character	ΔE^{vert} (f)	character	ΔE^{vert} (f)	character
1	4.20 (0.75)	Intra nBz	2.40 (0.49)	Deloc. Ind/nBz	2.70 (1.65)	Deloc. Ind/nBz
2	4.04 (0.17)	Bzt to nBz + Intra nBz	2.46 (0.92)	nBz to Bzt	3.78 (0.76)	nBz to Bzt
	4.11 (0.11)	Intra nBz				
3	4.38 (0.55)	Intra nPhol	3.03 (1.06)	Deloc. R_1/Ind	2.96 (1.06)	Deloc. R_1/Ind
	4.54 (0.68)	Intra R_1				
4	4.42 (0.48)	Intra nPhol	3.19 (0.94)	Intra nPhol	3.15 (1.00)	Deloc. R_1/Ind
5	3.78 (0.91)	Intra R_1	2.59 (1.15)	nPhol to Br + Ind	2.53 (1.71)	Deloc. R_1/Ind
			2.70 (0.50)	R_1 to Br + Ind		
6	4.43 (0.49)	Intra nPhol	3.61 (0.46)	Intra nPhol	4.29 (0.32)	Intra nPhol + nPhol to Ind
7	4.40 (0.49)	Intra nPhol	3.65 (0.50)	Intra nPhol	4.80 (0.22)	Intra nPhol
8	4.16 (0.83)	Intra R_1	2.69 (1.15)	Deloc. R_1/Ind + Ph to Deloc. R_1/Ind	2.65 (1.52)	Deloc. R_1/Ind
			2.81 (0.34)	Deloc. R_1/Ind + Ph to Deloc. R_1/Ind		
9	4.30 (0.74)	Intra nPhol + Ind. to nPhol	3.30 (1.16)	Deloc. R_1/Ind	3.26 (1.13)	Deloc. R_1/Ind
10	4.37 (0.63)	Ind to R_1 + intra R_1	3.27 (1.23)	Deloc. R_1/Ind	3.19 (1.20)	Deloc. R_1/Ind
11	3.46 (1.32)	Intra R_1	2.61 (1.95)	Deloc. R_1/Ind	2.50 (2.06)	Deloc. R_1/Ind
12	4.41 (0.51)	Intra nPhol + Intra R_1	2.81 (1.39)	Deloc. R_1/Ind	2.72 (1.45)	Deloc. R_1/Ind
	4.66 (0.99)	Intra R_1				

[a]Deloc: delocalized. nBz: substituted nitro-benzene. Bzt: benzothiazole/benzothiazolium. nPhol: nitro-phenol or nitro-phenolate. Ind: indoleninium. Br: CH_2=CH_2 bridge of R_1.

Table 7. Dynamic (1064 nm) Hyper-Rayleigh Scattering First Hyperpolarizabilities (β_{HRS}, au) and Depolarization Ratios (DR) of the Closed and Open Forms of Compounds 1−12 As Well As Their β_{HRS}(open)/β_{HRS}(closed) Contrast Ratios for the Photo- and Acido-Triggered Openings, As Obtained at the IEF-PCM/TDHF/6-311+G(d) Level (in Chloroform)

	closed (**a**)		open (**b**)		open (**b**$^+$)			
	β_{HRS}	DR	β_{HRS}	DR	β_{HRS}	DR	β_{HRS}(**b**)/β_{HRS}(**a**)	β_{HRS}(**b**$^+$)/β_{HRS}(**a**)
1	1442	4.79	13 375	4.57	15 044	4.69	9.28	10.43
2	661	3.19	9330	3.65	972	2.69	14.12	1.47
3	902	3.91	4770	5.93	3522	4.83	5.29	3.91
4	862	3.86	3681	6.01	2405	4.75	4.27	2.79
5	1764	3.78	20 298	5.17	22 927	4.84	11.51	13.00
6	790	3.30	1802	3.64	408	3.87	2.28	0.52
7	796	3.23	1959	3.68	425	3.79	2.46	0.53
8	1947	5.07	15 215	5.28	14 285	4.76	7.81	7.34
9	1310	2.92	1830	2.70	814	2.93	1.40	0.62
10	1015	2.81	2340	4.74	1239	4.60	2.31	1.22
11	3929	4.62	21 392	4.67	24 891	4.55	5.44	6.33
12	1437	4.58	11 652	4.89	13 499	4.71	8.11	9.39

strengths and the main character of the excitations. The corresponding simulated spectra as well as additional data are provided in the Supporting Information (Figure S7.1−S7.12). With the exception of compounds **5**, **8**, **10**, and **11** where they are localized on the R_1 substituent, the electronic excitations of the closed forms are localized on the nitro-phenol moiety and therefore the excitation energies are very similar. For the former, the excitation energies decrease in parallel with the donor character of R_1. In agreement with the results presented in the previous section, the excitation energy decreases upon opening. With the exception of compounds **6** and **7**, for a given R_1, the dominant low-energy band of the zwitterionic-open and protonated-open forms has a similar position. This is attributed to the same character of the excitations, which are delocalized over the indoleninium ring and the R_1 substituent. Nevertheless, the first band of the **b**$^+$ forms is slightly red-shifted with respect to that of the **b** forms, consistently with the larger electron conjugation along the vinylene linker, as indicated by the BLA values reported in Table 4. The ordering of the ΔE values for the forms **b** is **5** ∼ **11** < **8** < **12** < **3** < **4** < **10** ∼ **9** < **6** ∼ **7** whereas for forms **b**$^+$ it is **11** ∼ **5** < **8** < **12** < **3** < **4** < **10** < **9** < **6** < **7**. The smallest ΔE and largest f values are obtained for donor R_1 substituents and are similar to those of **1** and **2**. In the presence of acceptor groups, the excitation energies are larger and the oscillator strengths smaller. Compounds **3** and **4** exhibit intermediate ΔE values between those of compounds with substituents having donor and acceptor character. Finally, when R_1 = H or Ph, the excitation energies are even larger while the oscillator strengths do not change much with respect to the closed form. This is attributed to the lack of delocalization of the excitation. The simulated spectra (Figure S7.1−S7.12) also display the signatures of the nitro-phenol and nitro-phenolate groups with characteristic excitations close to 260 and 340 nm, respectively.

Static and dynamic HRS first hyperpolarizabilities and depolarization ratios are listed in Table 7 for the closed and

DOI: 10.1021/jacs.5b13243
J. Am. Chem. Soc. 2016, 138, 5052−5062

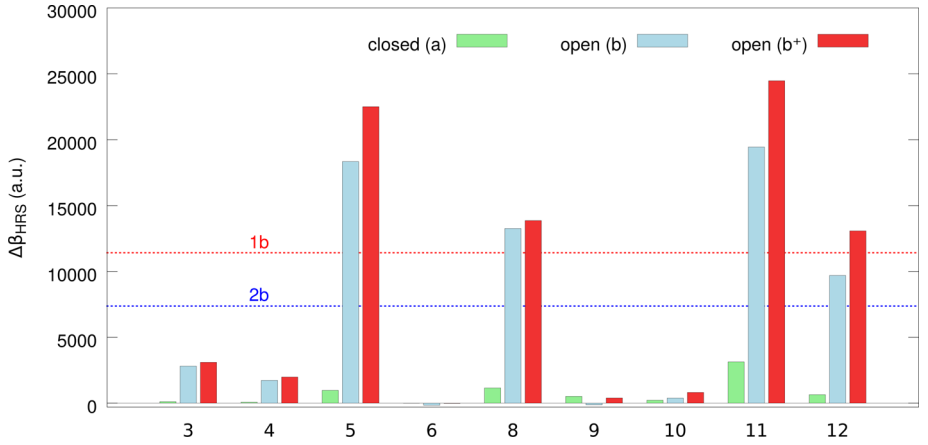

Figure 3. IEF-PCM/TDHF/6-311+G(d) dynamic (1064 nm) $\Delta\beta_{HRS}(X) = \beta^{X}_{HRS} - \beta^{7}_{HRS}$ for the closed (**a**), protonated ($\mathbf{b}^+$), and zwitterionic (**b**) open forms of **3**–**6** and **8**–**12** (in chloroform).

open forms of **1**–**12** together with their β_{HRS} contrasts for the two types of opening. Additional data are given in the Supporting Information (Tables S5 and S6). With the exception of **11a** where R_1 contains acceptor and donor chemical functions, the TDHF β_{HRS} of the closed forms are smaller than 2000 au, and even smaller than 1000 au for **3a** and **4a** (thiophene substituent) and for **6a** and **7a** (in which the R_1 substituent has no donor or acceptor character). The oxazine β_{HRS} responses are similar to those of the reference compounds (**1a** and **2a**). For most compounds the octupolar component of β is larger than the dipolar part (DR < 4.26 or ρ > 1).

Phototriggered opening of the oxazine leads to an increase of β_{HRS} that goes from 40% (**9**) to 1050% (**5**). This broad range of $\beta_{HRS}(\mathbf{b})/\beta_{HRS}(\mathbf{a})$ contrasts originates from the nature of the substituent. So, donor substituents in **5** and **8** lead to large β_{HRS} responses and therefore to large $\beta_{HRS}(\mathbf{b})/\beta_{HRS}(\mathbf{a})$ contrasts, which go together with a strong reduction of the BLA, a larger opening-induced charge transfer, and a smaller excitation energy. On the other hand, the contrast ratios are much smaller when R_1 is an acceptor group (**9** and **10**) or a small substituent (**6**, **7**). Compounds **3** and **4** with thiophene rings present intermediate enhancement ratios. Opening the oxazine to gain the $\mathbf{b}^+$ forms is also associated with a substantial increase of β_{HRS} with respect to the closed form when R_1 is a donor group. The situation is more contrasted for the other compounds. For compounds **6**, **7**, and **9**, β_{HRS} decreases whereas it increases slightly for compound **10**. In the case of the thiophene-containing compounds, β_{HRS} increases but less than in the case of the phototriggered open forms. Note that reference compounds **1** and **2** also display a substantial β_{HRS} increase upon forming the open zwitterionic forms, but in the case of its protonated form, the $\beta_{HRS}(\mathbf{b}^+)/\beta_{HRS}(\mathbf{a})$ contrast ratio for **2** is much smaller. This is attributed to a large change of geometry, corresponding to the increase of the torsion angle between the rings, from 29.1° (**2b**) to 43.6° ($\mathbf{2b}^+$). It is interesting to note that, although the excitation energies are not the only factor governing β, as shown in the sum-over-state Orr–Ward–Bishop expression,[27] the ordering of the β_{HRS} values is indeed almost opposite to that of the ΔE: for the **b** forms it is **11** ~ **5** > **8** > **12** > **3** > **4** > **10** > **7** > **9** ~ **6**, whereas, for the forms $\mathbf{b}^+$, it is **11** ~ **5** > **8** ~ **12** > **3** > **4** > **10** > **9** > **7** ~ **6**. Still, owing to the more complex effect of the substituent on β_{HRS} of the closed form, the orderings for the $\beta_{HRS}(\mathbf{b})/\beta_{HRS}(\mathbf{a})$ and $\beta_{HRS}(\mathbf{b}^+)/\beta_{HRS}(\mathbf{a})$ contrast ratios are different: **5** > **12** > **8** > **11** ~ **3** > **4** > **7** ~ **10** ~ **6** > **9** for phototriggered opening and **5** > **12** > **8** > **11** > **3** > **4** > **10** > **9** > **7** ~ **6** for acido-triggered opening. Nevertheless, the compounds can be classified in three main groups, those with donor substituents (**5**, **8**, **11**, and **12**), those with thiophene units (**3** and **4**), and those with acceptor or small substituents (**6**, **7**, **9**, and **10**). This explains our selection of four compounds, **3**, **4**, **11**, and **12**, for the experimental investigation. Upon opening DR generally increases and becomes larger than 4.26, demonstrating a dominant dipolar contribution to β_{HRS}. Compounds **6**, **7**, and **9** are exceptions to this.

Besides HF calculations, β_{HRS} of the **a**, **b**, and $\mathbf{b}^+$ forms of compounds **3**, **4**, **11**, and **12** were also evaluated at the MP2 level using the FF procedure (Table S3). A nice linear relationship between the MP2 and HF static β_{HRS} was obtained [β_{HRS}(MP2) = −1266 + 2.70 × β_{HRS}(HF)], leading to enhancement of the $\beta_{HRS}(\mathbf{b})/\beta_{HRS}(\mathbf{a})$ and $\beta_{HRS}(\mathbf{b}^+)/\beta_{HRS}(\mathbf{a})$ contrasts with respect to HF (besides for compounds **6** and **7**).

The substituent–substrate synergy effect was then quantified by referring to the $\Delta\beta_{HRS}$ quantity, defined as the β_{HRS} difference with respect to the oxazine **7**, where R_1 = H (Figure 3). While $\Delta\beta_{HRS}$ is small for the closed forms, it is exalted for the open forms, especially when R_1 is a donor group, π-conjugated to the indoleninium ring, highlighting π-conjugation and charge transfer between the two entities.

A complement to analyze the β_{HRS} responses of the **b** and $\mathbf{b}^+$ forms as a function of R_1 consists of considering the open forms as built from two NLOphores, a substituted indoleninium and nitrophenol ($\mathbf{b}^+$) or nitrophenolate (**b**). Then, since β_{HRS} of phenolate is larger than that of phenol, 2442 au versus 647 au as evaluated at the IEFPCM(acetonitrile)/TDHF(λ = 1064 nm)/6-311+G(d) level, its combination with the substituted indoleninium might lead to a decrease or an increase of β_{HRS} as a function of the donor or acceptor strength of R_1 as well as of the relative orientation of the two moieties. For acceptor R_1, the β-polarity of indoleninium and phenol(ate) is opposite, leading to partial cancellation of β_{HRS}. On the other hand for donor substituents, the two NLOphores are in-phase, leading to larger β_{HRS}. Still, there might be partial cancellation or damping of the β_{HRS} response owing to the relative orientation of the two moieties and to inter-NLOphore electrostatic interactions, as those found in aggregates or molecular crystals. Indeed, packing chromophores in the direction perpendicular to the dominant β component usually leads to reduction of β per unit.[38] This was

DOI: 10.1021/jacs.5b13243
J. Am. Chem. Soc. 2016, 138, 5052–5062

substantiated in the case of **3b** and **3b**$^+$. Indeed, their IEFPCM(acetonitrile)/TDHF(λ = 1064 nm)/6-311+G(d) β_{HRS} responses amount to 4292 and 3191 au whereas the sums of the β_{HRS} values of their components are 32% and 21% larger (5654 and 3859 au), respectively.

4. CONCLUSIONS AND OUTLOOK

A combined experimental−theoretical investigation has revealed that oxazine derivatives are efficient second-order NLO molecular switches, in particular when their substituent is a donor group. In this study, the cleavage of the C−O bond at the junction of the indole and oxazine cycles (of the closed **a** forms) is triggered by pH reduction, leading to a protonated open form (**b**$^+$) characterized by larger first hyperpolarizabilities (β_{HRS}) and smaller excitation energies than the closed form. These results are confirmed and interpreted utilizing *ab initio* calculations that have been carried out beforehand on a broader set of compounds to unravel the role of donor and acceptor substituents on the linear and nonlinear optical properties as well as on structural, electronic, and thermodynamical properties and therefore to select four representative species for an experimental−theoretical characterization. These have highlighted that donor groups are characterized by larger β_{HRS} and β_{HRS} contrast ratios, smaller excitation energies, larger opening-induced charge transfer and reduction of the bond length alternation, and smaller Gibbs energies of opening than in the case of acceptor groups. Calculations have also extended the study to the zwitterionic-open forms (**b**), pointing out similarities in the long-wavelength UV/vis absorption spectra of both (**b** and **b**$^+$) open forms whereas their β_{HRS} values might strongly differ as a function of the nature of the substituent. The latter effect has been attributed to the presence of two molecular moieties contributing to the first hyperpolarizability of the open forms and to the fact that the nitrophenol moiety (present in the protonated-open form, **b**$^+$) presents a smaller β_{HRS} response than its deprotonated nitrophenolate (present in the zwitterionic open form, **b**) analog. Together with previous studies on the optical responses as well as on redox- and photochemical-triggering, the present work demonstrates the multiaddressable, multistate, and multifunctional character of oxazine-based molecular switches.

■ ASSOCIATED CONTENT

Supporting Information

The Supporting Information is available free of charge on the ACS Publications website at DOI: 10.1021/jacs.5b13243.

Experimental UV/vis absorption spectra of the closed and protonated open forms of **3**, **4**, **11**, and **12** recorded in chloroform together with characteristics of their main low-energy bands and frequency dispersion factors; Simulated UV/vis absorption spectra of the closed and open forms of compounds **1**−**12** together with the excitation energies, oscillator strengths, and molecular orbitals involved in the major singly excited determinants for the dominant low-energy transitions; Parameters of the linear regression relationships between the experimental and simulated UV/vis absorption spectra of compounds **3**, **4**, **11**, and **12** in their closed and protonated open forms; HRS power and polarization scans of the closed and protonated open forms of **3**, **4**, **11**, and **12**; first hyperpolarizabilities of the protonated open and closed forms of compounds **1**−**12** as calculated at different levels of approximation and their contrast ratios; Spatial distribution on the S_1−S_5 and R_1 molecular moieties of the Mulliken, Hirshfeld, and NPA charge distributions and their variations for the closed, zwitterionic, and protonated open forms of compounds **1**−**12**; Cartesian coordinates and absolute energies of all compounds (PDF)

■ AUTHOR INFORMATION

Corresponding Author

*benoit.champagne@unamur.be

Notes

The authors declare no competing financial interest.

■ ACKNOWLEDGMENTS

This work was supported by funds from the Belgian Government (IUAP No P7/5 "Functional Supramolecular Systems"), the Francqui Foundation, by grants from the ANR (PHOEBUS) and the National Science Foundation (CHE-1049860). It has also been done in the frame of the Centre of Excellence LAPHIA (Investments for the future: Programme IdEx Bordeaux − LAPHIA (ANR-10-IDEX-03-02)). V.R. is grateful to F. Adamietz for HRS experimental support and technical developments as well as to the CNRS and the Région Aquitaine for funding supports. We thank V. Liégeois for the use of DrawMol, employed to make the TOC. The calculations were performed on the computers of the Consortium des Équipements de Calcul Intensif, including those of the Technological Platform of High-Performance Computing, for which we gratefully acknowledge the financial support of the FNRS-FRFC (Convention Nos. 2.4.617.07.F and 2.5020.11) and of the University of Namur, as well as on zenobe, the Tier-1 facility of the Walloon Region (Convention 1117545).

■ REFERENCES

(1) (a) Berkovic, G.; Krongauz, V.; Weiss, V. *Chem. Rev.* **2000**, *100*, 1741−1754. (b) Bouas-Laurent, H.; Dürr, H. *Pure Appl. Chem.* **2001**, *73*, 639−665. (c) Cusido, J.; Deniz, E.; Raymo, F. M. *Eur. J. Org. Chem.* **2009**, *2009*, 2031−2045. (d) Feringa, B. L., Browne, W. R., Eds. *Molecular Switches*, 2nd ed.; Wiley-VCH: Weinheim, 2011. (e) Zhang, J.; Zou, Q.; Tian, H. *Adv. Mater.* **2013**, *25*, 378−399.

(2) (a) Coe, B. J. *Chem. - Eur. J.* **1999**, *5*, 2464−2471. (b) Delaire, J. A.; Nakatani, K. *Chem. Rev.* **2000**, *100*, 1817−1845. (c) Castet, F.; Rodriguez, V.; Pozzo, J.-L.; Ducasse, L.; Plaquet, A.; Champagne, B. *Acc. Chem. Res.* **2013**, *46*, 2656−2665.

(3) Okuno, K.; Shigeta, Y.; Kishi, R.; Nakano, M. *J. Phys. Chem. Lett.* **2013**, *4*, 2418−2422.

(4) (a) Kanis, D. R.; Ratner, M. A.; Marks, T. J. *Chem. Rev.* **1994**, *94*, 195−242. (b) Brédas, J. L.; Adant, C.; Tackx, P.; Persoons, A.; Pierce, B. M. *Chem. Rev.* **1994**, *94*, 243−278. (c) Verbiest, T.; Houbrechts, S.; Kauranen, M.; Clays, C.; Persoons, A. *J. Mater. Chem.* **1997**, *7*, 2175−2189. (d) *Nonlinear Optical Properties of Matter: From Molecules to Condensed Phases*; Papadopoulos, M. G., Leszczynski, J.; Sadlej, A. J., Eds.; Springer: Dordrecht, 2006. (e) Murugan, N. A.; Kongsted, J.; Rinkevicius, Z.; Ågren, H. *Proc. Natl. Acad. Sci. U. S. A.* **2010**, *107*, 16453−16458. (f) Johnson, L. E.; Dalton, L. R.; Robinson, B. H. *Acc. Chem. Res.* **2014**, *47*, 3258−3265.

(5) Loucif-Saïbi, R.; Nakatani, K.; Delaire, J.; Dumont, M.; Sekkat, Z. *Chem. Mater.* **1993**, *5*, 229−236.

(6) (a) Gilat, S. L.; Kawaï, S. H.; Lehn, J. M. *Chem. - Eur. J.* **1995**, *1*, 275−284. (b) Aubert, V.; Guerchais, V.; Ishow, E.; Hoang-Thi, K.; Ledoux, I.; Nakatani, K.; Le Bozec, H. *Angew. Chem., Int. Ed.* **2008**, *47*, 577−580.

(7) Houbrechts, S.; Clays, K.; Persoons, A.; Pikramenou, Z.; Lehn, J.-M. *Chem. Phys. Lett.* **1996**, *258*, 485−489.

DOI: 10.1021/jacs.5b13243
J. Am. Chem. Soc. 2016, 138, 5052−5062

(8) (a) Nakatani, K.; Delaire, J. A. *Chem. Mater.* **1997**, *9*, 2682−2684. (b) (a) Sliwa, M.; Létard, S.; Malfant, I.; Nierlich, M.; Lacroix, P. G.; Asahi, T.; Masuhara, H.; Yu, P.; Nakatani, K. *Chem. Mater.* **2005**, *17*, 4727−4735. (c) Bogdan, E.; Plaquet, A.; Antonov, L.; Rodriguez, V.; Ducasse, L.; Champagne, B.; Castet, F. *J. Phys. Chem. C* **2010**, *114*, 12760−12768.
(9) (a) Coe, B. J.; Houbrechts, S.; Asselberghs, I.; Persoons, A. *Angew. Chem., Int. Ed.* **1999**, *38*, 366−369. (b) Averseng, F.; Lepetit, C.; Lacroix, P. G.; Tuchagues, J. P. *Chem. Mater.* **2000**, *12*, 2225−2229. (c) Asselberghs, I.; Clays, K.; Persoons, A.; McDonagh, A. M.; Ward, M. D.; McCleverty, J. A. *Chem. Phys. Lett.* **2003**, *368*, 408−411. (d) Aubert, V.; Guerchais, V.; Ishow, E.; Hoang-Thi, K.; Ledoux, I.; Nakatani, K.; Le Bozec, H. *Angew. Chem., Int. Ed.* **2008**, *47*, 577−580. (e) Boubekeur−Lecaque, L.; Coe, B. J.; Harris, J. A.; Helliwell, M.; Asselberghs, I.; Clays, K.; Foerier, S.; Verbiest, T. *Inorg. Chem.* **2011**, *50*, 12886−12899. (f) Green, K. A.; Cifuentes, M. P.; Samoc, M.; Humphrey, M. G. *Coord. Chem. Rev.* **2011**, *255*, 2530−2544. (g) Di Bella, S.; Oliveri, I. P.; Colombo, A.; Dragonetti, C.; Righetto, S.; Roberto, D. *Dalton Trans.* **2012**, *41*, 7013−7016. (h) Zhang, Y. R.; Castet, F.; Champagne, B. *Chem. Phys. Lett.* **2013**, *574*, 42−46. (i) Boixel, J.; Guerchais, V.; LeBozec, H.; Jacquemin, D.; Amar, A.; Boucekkine, A.; Colombo, A.; Dragonetti, C.; Marinotto, D.; Roberto, D.; Righetto, S.; De Angelis, R. *J. Am. Chem. Soc.* **2014**, *136*, 5367−5375. (j) Wang, W. Y.; Ma, N. N.; Sun, S. L.; Qiu, Y. Q. *Organometallics* **2014**, *33*, 3341−3352. (k) Boixel, J.; Guerchais, V.; Le Bozec, H.; Chantzis, A.; Jacquemin, D.; Colombo, A.; Dragonetti, C.; Marinotto, D.; Roberto, D. *Chem. Commun.* **2015**, *51*, 7805−7808.
(10) Asselberghs, I.; Zhao, Y.; Clays, K.; Persoons, A.; Comito, A.; Rubin, Y. *Chem. Phys. Lett.* **2002**, *364*, 279−283.
(11) (a) Sanguinet, L.; Pozzo, J.-L.; Rodriguez, V.; Adamietz, F.; Castet, F.; Ducasse, L.; Champagne, B. *J. Phys. Chem. B* **2005**, *109*, 11139−11150. (b) Mançois, F.; Pozzo, J.-L.; Adamietz, F.; Rodriguez, V.; Ducasse, L.; Castet, F.; Plaquet, A.; Champagne, B. *Chem. - Eur. J.* **2009**, *15*, 2560−2571. (c) Szaloki, G.; Alévêque, O.; Pozzo, J. L.; Hadji, R.; Levillain, E.; Sanguinet, L. *J. Phys. Chem. B* **2015**, *119*, 307−315. (d) Bondu, F.; Hadji, R.; Szalóki, G.; Alévêque, O.; Sanguinet, L.; Pozzo, J. L.; Cavagnat, D.; Buffeteau, T.; Rodriguez, V. *J. Phys. Chem. B* **2015**, *119*, 6758−6765.
(12) Giraud, M.; Léaustic, A.; Guillot, R.; Yu, P.; Lacroix, P. G.; Nakatani, K.; Pansu, R.; Maurel, F. *J. Mater. Chem.* **2007**, *17*, 4414−4425.
(13) Plaquet, A.; Guillaume, M.; Champagne, B.; Castet, F.; Ducasse, L.; Pozzo, J. L.; Rodriguez, V. *Phys. Chem. Chem. Phys.* **2008**, *10*, 6223−6232.
(14) (a) Plaquet, A.; Champagne, B.; Castet, F.; Ducasse, L.; Bogdan, E.; Rodriguez, V.; Pozzo, J.-L. *New J. Chem.* **2009**, *33*, 1349−1356. (b) Broman, S. L.; Jevric, M.; Bond, A. D.; Nielsen, M. B. *J. Org. Chem.* **2014**, *79*, 41−64.
(15) (a) Plaquet, A.; Champagne, B.; Kulhánek, J.; Bures, F.; Bogdan, E.; Castet, F.; Ducasse, L.; Rodriguez, V. *ChemPhysChem* **2011**, *12*, 3245−3252. (b) Bures, F.; Cermakova, A.; Kulhánek, J.; Ludwig, M.; Kuznik, W.; Kityk, I. V.; Mikysek, T.; Ruzicka, A. *Eur. J. Org. Chem.* **2012**, *2012*, 529−538.
(16) Cariati, E.; Dragonetti, C.; Lucenti, E.; Nisic, F.; Righetto, S.; Roberto, D.; Tordin, E. *Chem. Commun.* **2014**, *50*, 1608−1610.
(17) Castet, F.; Champagne, B.; Pina, F.; Rodriguez, V. *ChemPhysChem* **2014**, *15*, 2221−2224.
(18) van Bezouw, S.; Campo, J.; Lee, S. H.; Kwon, O. P.; Wenseleers, W. *J. Phys. Chem. C* **2015**, *119*, 21658−21663.
(19) Asselberghs, I.; Flors, C.; Ferrighi, L.; Botek, E.; Champagne, B.; Mizuno, H.; Ando, R.; Miyawaki, A.; Hofkens, J.; Van der Auweraer, M.; Clays, K. *J. Am. Chem. Soc.* **2008**, *130*, 15713−15719.
(20) (a) Tomasulo, M.; Sortino, S.; White, A. J. P.; Raymo, F. M. *J. Org. Chem.* **2005**, *70*, 8180−8189. (b) Deniz, E.; Tomasulo, M.; Cusido, J.; Sortino, S.; Raymo, F. M. *Langmuir* **2011**, *27*, 11773−11783. (c) Deniz, E.; Cusido, J.; Swaminathan, S.; Battal, M.; Impellizzeri, S.; Sortino, S.; Raymo, F. M. *J. Photochem. Photobiol., A* **2012**, *229*, 20−28. (d) Deniz, E.; Tomasulo, M.; Cusido, J.; Yildiz, I.; Petriella, M.; Bossi, M. L.; Sortino, S.; Raymo, F. M. *J. Phys. Chem. C* **2012**, *116*, 6058−6068. (e) Garcia-Amorós, J.; Swami-Nathan, S.; Raymo, F. M. *Dyes Pigm.* **2014**, *106*, 71−73.
(21) Zhu, S.; Li, M.; Tang, S.; Zhang, Y.-M.; Yang, B.; Zhang, S. X.-A. *Eur. J. Org. Chem.* **2014**, *2014*, 1227−1235.
(22) (a) Raymo, F. M. *J. Phys. Chem. A* **2012**, *116*, 11888−95. (b) Toliautas, S.; Sulskus, J.; Valkunas, L.; Vengris, M. *Chem. Phys.* **2012**, *404*, 64−73. (c) Redeckas, K.; Martynaitis, V.; Šačkus, A.; Vengris, M. *J. Photochem. Photobiol., A* **2014**, *285*, 7−15. (d) Redeckas, K.; Voiciuk, V.; Steponavičiute, R.; Martynaitis, V.; Šačkus, A.; Vengris, M. *J. Phys. Chem. A* **2014**, *118*, 5642−51.
(23) Verbiest, T.; Clays, K.; Rodriguez, V. *Second-Order Nonlinear Optical Characterization Techniques: An Introduction*; Taylor & Francis: Boca Raton, FL, 2009.
(24) (a) Castet, F.; Bogdan, E.; Plaquet, A.; Ducasse, L.; Champagne, B.; Rodriguez, V. *J. Chem. Phys.* **2012**, *136*, 024506. (b) Castet, F.; Blanchard-Desce, M.; Adamietz, F.; Poronik, Y. M.; Gryko, D. T.; Rodriguez, V. *ChemPhysChem* **2014**, *15*, 2575−81.
(25) Bersohn, R. *J. Chem. Phys.* **1966**, *45*, 3184−3198.
(26) (a) Oudar, J. L.; Chemla, D. S. *J. Chem. Phys.* **1977**, *66*, 2664−2668. (b) Campo, J.; Wenseleers, W.; Goovaerts, E.; Szablewski, M.; Cross, G. H. *J. Phys. Chem. C* **2008**, *112*, 287−296.
(27) (a) Orr, B.; Ward, J. *Mol. Phys.* **1971**, *20*, 513−526. (b) Bishop, D. M. *J. Chem. Phys.* **1994**, *100*, 6535−6542.
(28) Zhao, Y.; Truhlar, D. G. *Theor. Chem. Acc.* **2008**, *120*, 215−241.
(29) Li, R.; Zheng, J.; Truhlar, D. G. *Phys. Chem. Chem. Phys.* **2010**, *12*, 12697−12701.
(30) (a) Sekino, H.; Bartlett, R. J. *J. Chem. Phys.* **1986**, *85*, 976−989. (b) Karna, S. P.; Dupuis, M. *J. Comput. Chem.* **1991**, *12*, 487−504.
(31) (a) Champagne, B.; Kirtman, B. *J. Chem. Phys.* **2006**, *125*, 024101. (b) de Wergifosse, M.; Champagne, B. *J. Chem. Phys.* **2011**, *134*, 074113. (c) Hidalgo Cardenuto, M.; Champagne, B. *Phys. Chem. Chem. Phys.* **2015**, *17*, 23634−23642.
(32) Cohen, H. D.; Roothaan, C. C. J. *J. Chem. Phys.* **1965**, *43*, S34.
(33) (a) Mohammed, A. A. K.; Limacher, P. A.; Champagne, B. *J. Comput. Chem.* **2013**, *34*, 1497−1503. (b) de Wergifosse, M.; Liégeois, V.; Champagne, B. *Int. J. Quantum Chem.* **2014**, *114*, 900−910.
(34) (a) Sekino, H.; Bartlett, R. J. *J. Chem. Phys.* **1986**, *84*, 2726−2733. (b) Rice, J. E.; Handy, N. *Int. J. Quantum Chem.* **1992**, *43*, 91−118. (c) Sekino, H.; Bartlett, R. J. *Chem. Phys. Lett.* **1995**, *234*, 87−93. (d) Jacquemin, D.; Champagne, B.; Hättig, C. *Chem. Phys. Lett.* **2000**, *319*, 327−334.
(35) Willetts, A.; Rice, J. E.; Burland, D. M.; Shelton, D. P. *J. Chem. Phys.* **1992**, *97*, 7590−7599.
(36) (a) Mennucci, B.; Cammi, R.; Tomasi, J. *Int. J. Quantum Chem.* **1999**, *75*, 767−781. (b) Tomasi, J.; Mennucci, B.; Cammi, R. *Chem. Rev.* **2005**, *105*, 2999−3094.
(37) Frisch, M. J.; Trucks, G. W.; Schlegel, H. B.; Scuseria, G. E.; Robb, M. A.; Cheeseman, J. R.; Scalmani, G.; Barone, V.; Mennucci, B.; Petersson, G. A.; Nakatsuji, H.; Caricato, M.; Li, X.; Hratchian, H. P.; Izmaylov, A. F.; Bloino, J.; Zheng, G.; Sonnenberg, J. L.; Hada, M.; Ehara, M.; Toyota, K.; Fukuda, R.; Hasegawa, J.; Ishida, M.; Nakajima, T.; Honda, Y.; Kitao, O.; Nakai, H.; Vreven, T.; Montgomery, J. A., Jr.; Peralta, J. E.; Ogliaro, F.; Bearpark, M.; Heyd, J. J.; Brothers, E.; Kudin, K. N.; Staroverov, V. N.; Kobayashi, R.; Normand, J.; Raghavachari, K.; Rendell, A.; Burant, J. C.; Iyengar, S. S.; Tomasi, J.; Cossi, M.; Rega, N.; Millam, N. J.; Klene, M.; Knox, J. E.; Cross, J. B.; Bakken, V.; Adamo, C.; Jaramillo, J.; Gomperts, R.; Stratmann, R. E.; Yazyev, O.; Austin, A. J.; Cammi, R.; Pomelli, C.; Ochterski, J. W.; Martin, R. L.; Morokuma, K.; Zakrzewski, V. G.; Voth, G. A.; Salvador, P.; Dannenberg, J. J.; Dapprich, S.; Daniels, A. D.; Farkas, O.; Foresman, J. B.; Ortiz, J. V.; Cioslowski, J.; Fox, D. J. *Gaussian 09*, Revision D01; Gaussian, Inc.: Wallingford, CT, 2009.
(38) (a) Castet, F.; Champagne, B. *J. Phys. Chem. A* **2001**, *105*, 1366−1370. (b) Suponitsky, K. Y.; Masunov, A. E. *J. Chem. Phys.* **2013**, *139*, 094310.

DOI: 10.1021/jacs.5b13243
J. Am. Chem. Soc. 2016, 138, 5052−5062